Human Movement Science 93 (2024) 103179

Contents lists available at ScienceDirect

Human Movement Science

journal homepage: www.elsevier.com/locate/humov

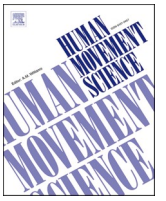

Estimation of sagittal-plane whole-body angular momentum during perturbed and unperturbed gait using simplified body models

J. Zhang [a,*], M. van Mierlo [b], P.H. Veltink [a], E.H.F. van Asseldonk [b]

[a] Department of Biomedical Signals and Systems, University of Twente, Enschede, the Netherlands
[b] Department of Biomechanical Engineering, University of Twente, Enschede, the Netherlands

ARTICLE INFO

Keywords:
Whole-body angular momentum
Segmental angular momentum contribution
Simplified body model
Perturbed gait

ABSTRACT

Human whole-body angular momentum (WBAM) during walking typically follows a consistent pattern, making it a valuable indicator of the state of balance. However, calculating WBAM is labor-intensive, where the kinematic data for all body segments is needed, that is, based on a full-body model. In this study, we focused on selecting appropriate segments for estimating sagittal-plane WBAM during both unperturbed and perturbed gaits, which were segments with significant angular momentum contributions. Those major segments were constructed as a simplified model, and the sagittal-plane WBAM based on a simplified model was calculated by combining the angular momenta of the selected segments. We found that the WBAM estimated by seven-segment models, incorporating the head & torso (HT) and all lower limb segments, provided an average correlation coefficient of 0.99 and relative angular momentum percentage of 96.8% and exhibited the most similar sensitivity to external perturbations compared to the full-body model-based WBAM. Additionally, our findings revealed that the rotational angular momenta (RAM) of lower limb segments were much smaller than their translational angular momenta (TAM). The pair-wise comparisons between simplified models with and without RAMs of lower body segments were observed with no significant difference, indicating that RAMs of lower body segments are neglectable. This may further simplify the WBAM estimation based on the seven-segment model, eliminating the need to estimate the angular velocities of lower limb segments. These findings have practical implications for future studies of using inertial measurement units (IMUs) for estimating WBAM, as our results can help reduce the number of required sensors and simplify kinematics measurement.

1. Introduction

During stable gait, the whole-body angular momentum (WBAM) with respect to the whole-body center of mass (CoM) appears to maintain a regular pattern about all three spatial directions. This is achieved through segment-to-segment cancellation (Herr & Popovic, 2008) and control of joint moments (van Mierlo, Ambrosius, Vlutters, van Asseldonk, & van der Kooij, 2022), resulting in little deviation of WBAM from zero throughout the gait cycle. Bennett, Russell, Sheth, & Abel, 2010 studied the influence of walking speeds on WBAM and found a decrease in the extrema of WBAM with increasing gait speeds. In addition to stable gait on level ground,

* Corresponding author.
E-mail address: j.zhang-7@utwente.nl (J. Zhang).

https://doi.org/10.1016/j.humov.2024.103179
Received 5 October 2023; Received in revised form 31 December 2023; Accepted 10 January 2024
Available online 21 January 2024

several studies have investigated how humans regulate their WBAM during various daily-life tasks, such as stair ascent and descent (Pickle, Wilken, Aldridge, Neptune, & Silverman, 2014; Silverman, Neptune, Sinitski, & Wilken, 2014), sloped walking (Pickle, Wilken, Aldridge Whitehead, & Silverman, 2016; Silverman, Wilken, Sinitski, & Neptune, 2012), 90-degree turns (Nolasco, Silverman, & Gates, 2019), etc. All these studies emphasized that the ability to regulate WBAM is crucial for maintaining balance during dynamic tasks.

Since the WBAM remains relatively regular with only small deviations during stable tasks (Herr & Popovic, 2008), any significant fluctuations in the WBAM may indicate a change in the state of balance. Therefore, there is a potential to quantify the state of balance by measuring the deviation of WBAM from its stable patterns. Exposure to perturbations (Brough, Klute, & Neptune, 2021; Martelli, Monaco, Bassi Luciani, & Micera, 2013; Miller, Segal, Klute, & Neptune, 2018; van Mierlo et al., 2022) can result in a changed state of balance. Additionally, there are many reasons that may affect the state of balance indirectly such as aging and diseases, as observed during stepping in old adults (Begue et al., 2021), in individuals with post-stroke (Honda, Sekiguchi, Muraki, & Izumi, 2019; Nott, Neptune, & Kautz, 2014), Parkinson's disease (Gomez, Foreman, Hunt, & Merryweather, 2022), transtibial amputation (Gaffney, Christiansen, Murray, & Davidson, 2017; Sheehan, Beltran, Dingwell, & Wilken, 2015), or cerebral palsy (Bruijn, Meyns, Jonkers, Kaat, & Duysens, 2011).

Unfortunately, calculating WBAM is a cumbersome task that requires precise measurements and calculations of the kinematics of each body segment. To date, optical motion capture systems are commonly used to calculate the WBAM based on a full-body model in lab settings (van Mierlo et al., 2022). However, these systems require a time-consuming process of placing reflective markers on anatomically relevant locations to track motion. They are also constrained to a limited capture volume (mostly indoors), and post-processing can be laborious. In comparison, wearable sensing systems, such as those utilizing inertial measurement units (IMUs), offer an economical, efficient, easy-to-use method and the possibility to perform in larger volumes than optical motion capture systems for collecting movement data in daily life settings. For daily-life usage, it is crucial that the system is easy to don and doff. However, commercial wearable sensing systems (Roetenberg, Luinge, Slycke, et al., 2009) often require a sensor to be placed on each body segment, resulting in >10 sensors that must be affixed to the person, making them impractical and inconvenient for daily life use. To address the issue of the inconvenience of current wearable sensing systems, a potential solution that is better feasible for daily life is to develop algorithms that require fewer sensors. Although this can increase ease of use, it results in an underdetermined system for estimating WBAM, as not all body segments can be tracked. Therefore, a simplified body model with a reduced number of segments should be used.

To determine the optimal set of segments for estimating WBAM, the contribution of each segment needs to be investigated. The segmental contribution analysis can aid in creating simplified models with only major contributing segments. Several previous studies have already investigated the contribution of segments during straight-line walking (Bennett et al., 2010; Bruijn, Meijer, van Dieën, Kingma, & Lamoth, 2008; Herr & Popovic, 2008) and stepping tasks (Begue et al., 2021). In daily-life conditions, exposure to various

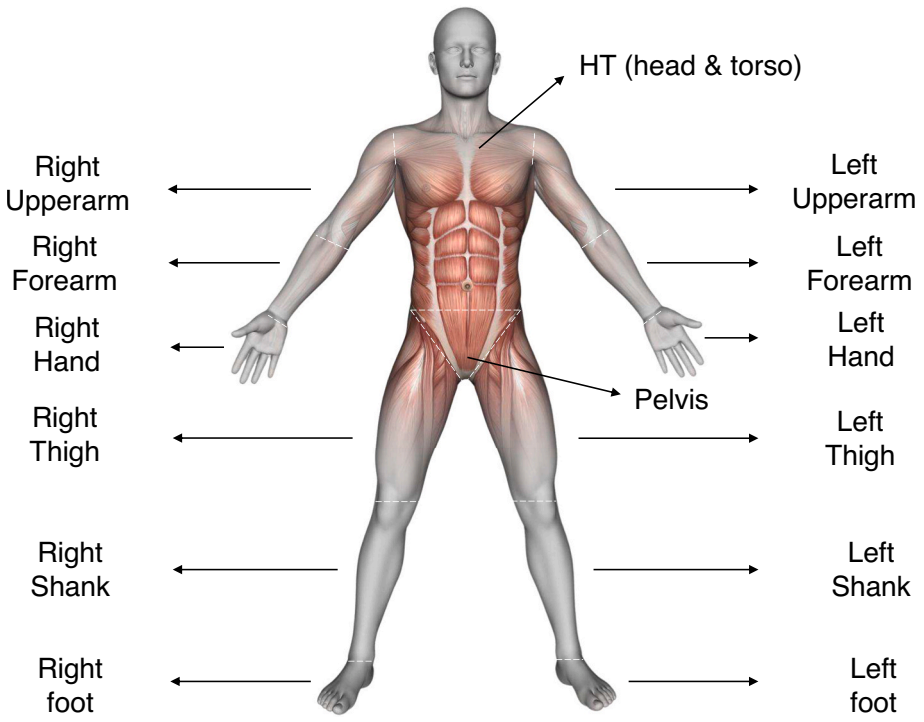

Fig. 1. Human body model with 14 segments, which was rearranged from the Opensim model with 22 bones. The background 3D male figure was downloaded from freepik, which contains a free license for commercial and personal projects.

kinds of perturbations can occur which lead to a change in the WBAM. Hence, investigating segmental angular momentum under perturbed conditions is also important, such as multidirectional slipping perturbations through treadmill acceleration and deceleration (Martelli et al., 2013) and foot-placement perturbations caused by tripping (Brough et al., 2021; Miller et al., 2018). Unfortunately, although the segmental angular momentum contribution was partly investigated in these studies, these perturbation methods do not only influence the WBAM. Also the whole-body linear momentum (WBLM) will be affected, which is proportional to the CoM velocity. This makes it difficult to isolate the analysis of segmental contributions in the regulation of the WBAM specifically.

Additionally, there is a lack of studies on the contribution of the separate components of the segmental angular momentum. The first component is the translational angular momentum (TAM) (Gaffney, Christiansen, Murray, Silverman and Davidson, 2017), resulting from the translation of the segment CoM relative to the whole-body CoM, where the relative velocity and position of the segment CoM with respect to the whole-body CoM should be measured, and the segment mass should be estimated using scaling procedures described such as by Zatsiorsky & Seluyanov, 1979, and modified by de Leva, 1996. Another component is the rotational angular momentum (RAM) (Gaffney et al., 2017), resulting from rotation about its own CoM, where the rotational inertia and the angular velocity of the segment are needed. An insightful analysis into TAM and RAM may simplify the required kinematic measurements and inertial parameter estimation of segments in future WBAM estimation. These limitations motivate us to provide a specific evaluation of segmental contributions to WBAM under the condition that only the WBAM is perturbed, by separating segmental angular momentum into TAM and RAM.

Based on the segmental contribution analysis, simplified body models with a reduced number of major contributing segments can

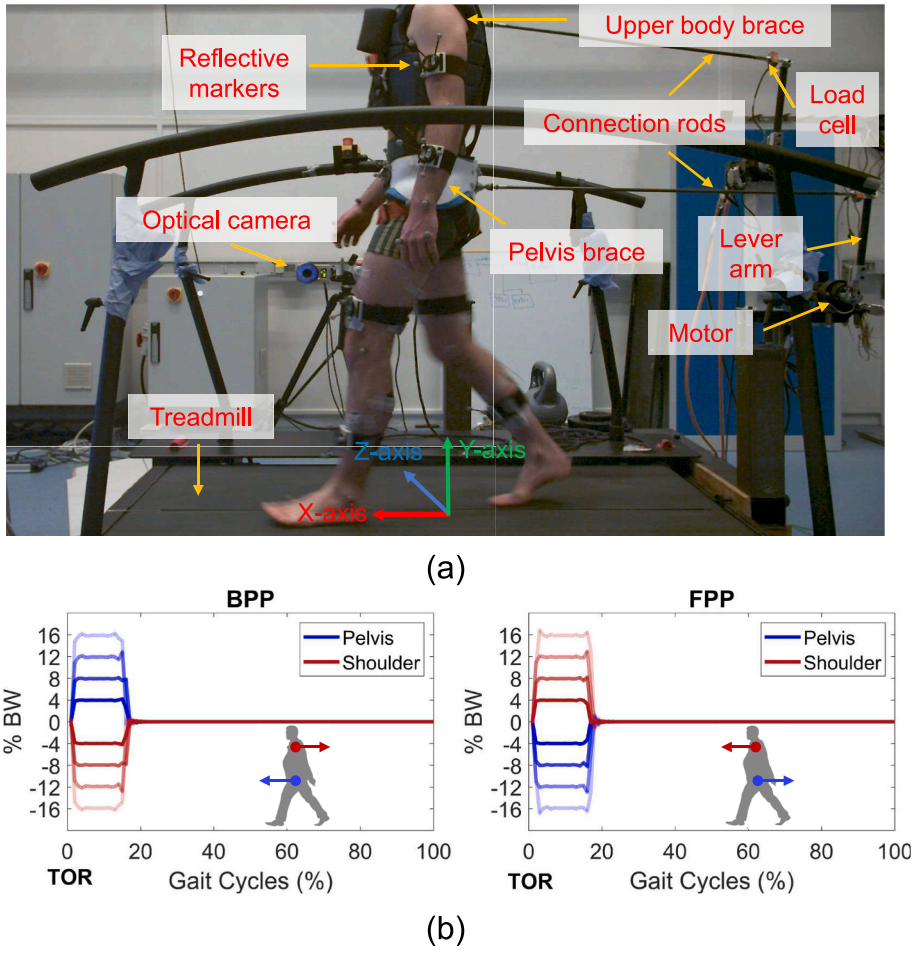

Fig. 2. (a) Experimental setup. The participants walked on the treadmill with a normal walking speed scaled to their leg length: $\sqrt{L} \cdot 1.25\mathrm{m/s}$, with L measured from the floor to the trochanter major while standing upright. (b) The experiment consisted of both unperturbed and perturbed parts. The unperturbed part consisted of 3 min of unperturbed walking. During the perturbed part, forward and backward pitch perturbations (FPP and BPP) were applied to the participants by using two motors to give simultaneous forces in opposite directions at the pelvis and upper body. FPP was defined as backward forces on the pelvis and forward forces on the upper body with equal magnitudes, and in the opposite direction for BPP. Both perturbations were given at the moment of toe-off right (TOR) and lasted for 150 ms. The forces generated by the two motors under different perturbation conditions were represented by % of the body weight (% BW). Positive(forward) forces were denoted if the forces were pointing in the positive direction of the X-axis.

be created. The next step is to investigate the performance of these models in estimating the WBAM compared to a full-body model that includes the segmental angular momenta of all body segments as shown in Fig. 1. To the best of our knowledge, there is a lack of adequate research in the current literature on this issue. A simplified model with seven body segments, including the upper body as one segment and six lower limb segments, was employed in the sagittal-plane foot placement estimator method (Millard, Wight, McPhee, Kubica, & Wang, 2009). However, the authors did not investigate whether this model could sufficiently capture WBAM. Liu et al., 2023 recently investigated a simplified model with seven segments for WBAM calculation. The model was created by merging several connected body segments. Their experiments for both people with and without lower extremity amputation showed that the simplified model was able to accurately calculate the WBAM in three self-selected walking speeds, normal, slow, and fast. However, only a qualitative analysis was provided, and the simplified model was only evaluated in unperturbed walking conditions. Therefore, the performance of simplified models in estimating WBAM also needs to be validated more quantitatively during both unperturbed and perturbed gaits.

Based on the above-mentioned limitations in the current literature, our main objective is to identify appropriate segments for estimating the sagittal-plane WBAM during both unperturbed and perturbed gaits. To achieve this goal, we selected several simplified models with a reduced number of major segments, based on an analysis of the segmental angular momenta to determine the set of segments with the most contributions. The sagittal-plane WBAM based on a simplified model was calculated by combining the angular momenta of the selected segments. The performance of these simplified models in estimating the sagittal-plane WBAM was subsequently evaluated quantitatively relative to a full-body model that includes the segmental angular momenta of all body segments as shown in Fig. 1.

2. Methods

2.1. Experimental setup

Ten healthy subjects (four males and six females, age 24 $\pm$ 3 years old, weight 66 $\pm$ 7 kg, height 1.75 $\pm$ 0.06 m, means $\pm$ standard deviation (SD)) were enrolled in the experiments. Research procedures were in accordance with the Declaration of Helsinki and were approved by the Local Ethical Committee (with the reference number RP 2019–88).

The experimental setup is shown in Fig. 2(a), which was the same as the one collected in our previous work for van Mierlo et al., 2022. Participants walked on the treadmill (custom Y-Mill, Motek medical, Culemborg, The Netherlands) with integrated force plates during the experiments. Sagittal-plane WBAM perturbations were provided by two motors generating simultaneous forces applied at the pelvis and upper body in opposite directions. Horizontal rods were connected to the participant's body via a brace worn around the pelvis and upper body. Load cells (Model LRF350, FUTEK, Los Angeles, CA, USA) were integrated in the horizontal rods to measure and minimize the interaction forces during walking and to track the desired forces at the instant a perturbation was given via an admittance controller (described by van der Kooij et al., 2022). By using these two motors to give simultaneous forces in opposite directions, this setup enabled the ability to apply perturbations of mainly the WBAM. The participants wore a safety harness connected to a fall protection system at the ceiling. The 3-D kinematics of the participants was recorded using an eight-camera-based motion capture system (Oqus 600+, Qualisys, Göteborg, Sweden) with a sample rate of 128 Hz. Data from the load cells was recorded at 1000 Hz and synchronized with the kinematic data via a synchronization signal.

2.2. Experimental protocol

The participants walked on the treadmill with a normal walking speed scaled to their leg length: $\sqrt{L} \cdot 1.25\mathrm{m/s}$, with L measured from the floor to the trochanter major while standing upright. The scaled normal walking speed was transferred to $\mathrm{km/h}$ to be set in the control panel of the treadmill. The experiment consisted of both unperturbed and perturbed parts. The unperturbed part consisted of 3 min of unperturbed walking. During the perturbed part, forward and backward pitch perturbations (FPP and BPP) were applied to the participants. As shown in Fig. 2(b), FPP was defined as backward forces on the pelvis and forward forces on the upper body with equal magnitudes, and BPP was defined in the opposite direction. The magnitudes of the given forces for BPP and FPP conditions were 4, 8, 12, or 16% of the body weight (BW). All perturbations were given at the moment of toe-off right (TOR) and lasted for 150 ms. Each perturbation condition was repeated 6 times during each recording session in a random order, with a random interval ranging from 3 to 6 strides between subsequent perturbations to avoid anticipation. During both unperturbed and perturbed parts, the participants were instructed to walk with their arms along their body with a free arm swing and without grasping the railing of the treadmill.

2.3. Data processing

Processing of the data was done with Matlab (R2021b, MathWorks). A full-body model consisting of 22 bones was scaled for each participant using OpenSim 4.2 (Rajagopal et al., 2016). In this paper, we combined several bones of the 22-bones OpenSim model together in one segment, resulting in effectively 14 segments, as shown in Fig. 1. They were HT (head & torso), pelvis, lower limb segments including right and left thighs, shanks, and feet, and upper limb segments including upper arms, forearms, and hands.

The WBAM with respect to the whole-body CoM was calculated by (1) where j represented each body segment,

$$\boldsymbol{H}_{\text{full}} = \sum_{j=1}^{14} \boldsymbol{H}_j = \sum_{j=1}^{14} \left[\overbrace{m_j\left(\boldsymbol{r}_{\text{CoM},j} - \boldsymbol{r}_{\text{CoM}}\right) \times \left(\boldsymbol{v}_{\text{CoM},j} - \boldsymbol{v}_{\text{CoM}}\right)}^{\text{TAM}} + \overbrace{\boldsymbol{I}_j\boldsymbol{\omega}_j}^{\text{RAM}} \right] \tag{1}$$

where $\boldsymbol{H}_{\text{full}}$ is the WBAM, $\boldsymbol{H}_j$ is the segmental angular momentum of j-th segment, $\boldsymbol{r}_{\text{CoM},j}$ and $\boldsymbol{r}_{\text{CoM}}$ are the positions of j-th segment and the whole-body CoM, respectively, and $\boldsymbol{\omega}_j$ represents the angular velocity of each segment. $\boldsymbol{r}_{\text{CoM},j}$ and $\boldsymbol{r}_{\text{CoM}}$ are the velocities of j-th segment and the whole-body CoM. Whole-body CoM position and velocity were calculated as the mass-weighted sum of the CoM positions and velocities of all segments. Body segment inertial parameters (i.e., mass m_j, CoM position $\boldsymbol{r}_{\text{CoM},j}$, and inertia tensor $\mathbf{I}_j$ with respect to its CoM) were calculated using procedures described by Zatsiorsky & Seluyanov, 1979 and modified by de Leva, 1996. The angular momentum $\boldsymbol{H}_j$ is composed of two separate components (Gaffney et al., 2017): TAM, the first term in (1), resulting from the rotation of the segment relative to the whole-body CoM $\boldsymbol{r}_{\text{CoM}}$, and RAM, the second term in (1), resulting from rotation about its $\boldsymbol{r}_{\text{CoM},j}$. The WBAM and segmental angular momenta were normalized for individual participants by dividing them through a scaling factor based on the participant's mass (M, kg), walking speed (V, m/s), and leg length (L, m), resulting in a unitless angular momentum measure. All measures are given in the global coordinate system defined in Fig. 1(a).

Since only sagittal-plane angular momentum perturbations were considered, we only analysed the sagittal-plane WBAM and segmental angular momenta. The sagittal-plane angular momentum was defined as the component of the 3-D angular momentum vectors $\boldsymbol{H}_{\text{full}}/\boldsymbol{H}_j$ in (1) along the mediolateral axis (the Z axis of the global coordinate system used in this paper), which is shown in Fig. 3. We used scalar notations of H_{full} and H_j to denote the sagittal-plane WBAM and segmental angular momenta in the following analysis, which was defined as

$$\begin{aligned} H_{\text{full}} &= H_{\text{full}} e_z^T \\ H_j &= H_j e_z^{\text{T}} \end{aligned} \tag{2}$$

where $e_z = [0, 0, 1]$, representing that we extracted the sagittal-plane angular momentum. During perturbed conditions, only the perturbed stride for each perturbation trial was evaluated. All angular momenta were interpolated over time by resampling each stride cycle to 100 samples. This allowed for averaging the data over all repetitions within each participant and across all participants.

2.4. Evaluation method

In order to select segments for inclusion in simplified body models, we first investigated the angular momentum contribution of

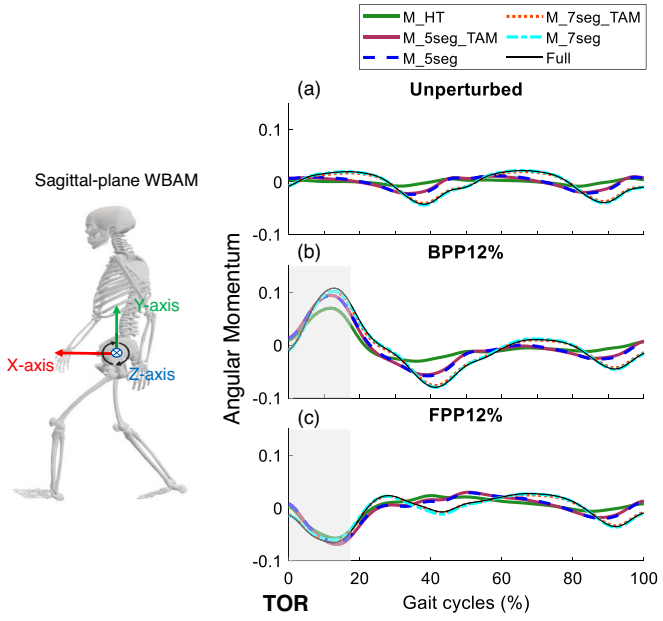

Fig. 3. Averaged normalized sagittal-plane whole-body angular momentum (WBAM) across all repetitions and subjects for the full-body model and the simplified models listed in Table 1. The gray shaded area is the perturbation period. Three subfigures show the angular momenta under the unperturbed (a), BPP 12% (b), and FPP 12% (c). The sagittal-plane angular momentum was defined as the component of the 3-D angular momentum vectors $\boldsymbol{H}_{\text{full}}/\boldsymbol{H}_j$ in (1) along the mediolateral axis (the Z axis of the global coordinate system used in this paper). The forward pitch perturbations (FPP) were defined as backward forces on the pelvis and forward forces on the upper body with equal magnitudes (represented by % of the body weight, % BW), and in the opposite direction for backward pitch perturbations (BPP). Perturbations were given at the moment of toe-off right (TOR) and lasted for 150 ms with the gray shaded area representing the perturbation period.

each segment in the WBAM, using both Pearson's correlation coefficients $\rho_{seg,k}^{\text{overall}}$, $\rho_{seg,k}^{\text{RAM}}$, $\rho_{seg,k}^{\text{TAM}}$ and relative angular momentum percentages $perc_{seg,k}^{\text{overall}}$, $perc_{seg,k}^{\text{RAM}}$, $perc_{seg,k}^{\text{TAM}}$ as evaluation metrics. Evaluation metrics are detailed in Appendix A. Only segments with major contributions in both unperturbed and perturbed gaits were chosen, that is, they should have both high correlation coefficients ($\rho_{seg,k}^{\text{overall}}$) and relative angular momentum percentages ($perc_{seg,k}^{\text{overall}}$). Simplified models were constructed by a combination of those segments with major contributions. The separation analysis of the contributions of the TAM and RAM aimed to identify whether it is necessary to include both TAM and RAM of the selected segment or solely one of them. The angular momentum of the simplified model i was calculated by combining the angular momenta of the selected segments, which was defined as

$$H_{\text{model},i} = \left\{ \sum_{j \in \mathbf{S}} a_j \cdot \overbrace{m_j\left(\boldsymbol{r}_{\text{CoM},j} - \boldsymbol{r}_{\text{CoM}}\right) \times \left(\boldsymbol{v}_{\text{CoM},j} - \boldsymbol{v}_{\text{CoM}}\right)}^{\text{TAM}} + \sum_{j \in \mathbf{S}} b_j \cdot \overbrace{\boldsymbol{I}_j \boldsymbol{\omega}_j}^{\text{RAM}} \right\} e_z^{\text{T}} \tag{3}$$

where $\mathbf{S}$ is the selected set of segments, $a_j \in \{0,1\}, b_j \in \{0,1\}$ with '1' including TAM/RAM of the segment, '0' denoting without including the component. In this paper, the position $\boldsymbol{r}_{\text{CoM}}$ and velocity $\boldsymbol{v}_{\text{CoM}}$ of the whole-body CoM used in computing the WBAM based on the simplified models were the same as the values computed from the full-body model.

Within one stride cycle, the performance of different simplified models in estimating the sagittal-plane WBAM during perturbed and unperturbed gait was evaluated by means of Pearson's correlation coefficients $\rho_{\text{model},i}$ (difference in the signal pattern similarity), and the median of the relative angular momentum percentage (difference in the signal magnitude) between the angular momentum of the simplified model and the full-body WBAM, defined as $perc_{\text{model},i}$,

$$perc_{\text{model},i} = \underset{t=1,2,\ldots,100}{Median}\left[\frac{H_{\text{model},i}(t)}{H_{\text{full}}(t)}\right] \times 100\% \tag{4}$$

In addition, we added a measure to evaluate whether the simplified models were as sensitive to perturbations as the full-body model, called incremental perturbation sensitivity. Within one stride cycle, the ranges of sagittal-plane WBAM of each simplified model under both unperturbed and different perturbation conditions were calculated. The range was defined as the difference between maximum and minimum values of the estimated sagittal-plane WBAM for each simplified model. By taking the range of each simplified model under the unperturbed condition as the baseline, the incremental perturbation sensitivity under different perturbation conditions was defined as

$$incre_{\text{model},i}(\%) = \frac{H_{\text{model},i}^{\text{range}}[perturbed] - H_{\text{model},i}^{\text{range}}[unperturbed]}{H_{\text{model},i}^{\text{range}}[unperturbed]} \times 100\% \tag{5}$$

The incremental perturbation sensitivity of the full-body model was also calculated for comparison.

2.5. Analysis of results

Firstly, for each unperturbed and perturbed condition, all evaluation metrics of the segments and simplified models were evaluated across all repetitions and subjects, and presented as mean ± SD.

Secondly, to test the effect of the choice of different simplified models on the estimated sagittal-plane WBAM, we performed nonparametric one-way repeated ANOVAs with the choice of simplified models as the main effect to compare evaluation metrics between models. The Friedman test (Friedman, 1940) was used since these evaluation metrics were not normally distributed. Post-hoc contrasts followed the Dunn's Test (Dunn, 1964) and were tested for pair-wise differences between models, and the significance was assessed at a α level of 0.05. It should be noted that we cannot do pair-wise comparisons between the full-body model and simplified models in $\rho_{\text{model},i}$ and $perc_{\text{model},i}$ since the full-body model always has the largest $\rho_{\text{model},i}$ (1.0) and $perc_{\text{model},i}$ (100%) without any variations. The statistical analysis was performed in GraphPad Prism 10.0.2 (GraphPad Software, Boston, USA).

A simplified model was considered to effectively estimate the WBAM if it had high $\rho_{\text{model},i}$ (close to 1) and $perc_{\text{model},i}$ (close to 100%), and exhibited similar $incre_{\text{model},i}$ compared to the full-body model.

3. Results

Our segmental contribution results in Appendix B indicated that the upper limb and pelvis segments had much lower contributions to WBAM than the HT segment and lower limb segments across all unperturbed and perturbed conditions. The pelvis's RAM and TAM were low due to its small angular velocity, and its small distance and velocity differences relative to the whole-body CoM, respectively. The masses and inertia tensors of the upper limb segments were relatively smaller than the HT segment and lower limb segments, which resulted in their limited contributions to the sagittal-plane WBAM. Therefore, the HT segment and lower limb segments were major contributing segments, thus the set of the selected segments is $\mathbf{S}\rightarrow$\{HT segment (including the pelvis), thighs, shanks, feet\}. It is noted that although the pelvis had a low contribution, it should not be ignored in the simplified model since it is important to reconstruct the whole-body kinematics. The mass of the pelvis was merged into the HT segment, and the CoM position and velocity of the merged HT segment were calculated from the mass-weighted sum of the CoM positions and velocities of the pelvis and original HT segment. The inertia tensor of the merged HT segment was calculated with respect to the modified CoM. The angular velocity of the

merged HT segment was appointed as the angular velocity of the original HT segment. Table 1 displays several potential simplified models derived from the selected set of segments. Furthermore, our results showed that the TAMs of lower limb segments contributed the most to segmental angular momenta, regardless of whether the conditions were perturbed or not. Therefore, in the following analysis, we included simplified models with (M_5seg and M_7seg models) and without (M_5seg_TAM and M_7seg_TAM models) the RAMs of lower limb segments to test whether the RAMs of lower limb segments could be ignored. The angular momenta of the simplified models listed in Table 1 were calculated by (3).

Fig. 3 shows the angular momenta of the full-body model and simplified models under the unperturbed, BPP 12%, and FPP 12% conditions, which were averaged and normalized across all repetitions and subjects. $\rho_{\text{model},i}$, $perc_{\text{model},i}$ and $incre_{\text{model},i}$ of the full-body model and simplified models during perturbed and unperturbed conditions are shown in Figs. 4–6, respectively.

Comparisons of $\rho_{\text{model},i}$, $perc_{\text{model},i}$ and $incre_{\text{model},i}$ between the full-body model and different simplified models showed remarkable variations, as demonstrated in Figs. 4–6. The M_7seg_TAM and M_7seg models exhibited an average $\rho_{\text{model},i}$ and $perc_{\text{model},i}$ of 0.99 (Fig. 4) and 96.8% (Fig. 5), respectively, across all conditions. The average $\rho_{\text{model},i}$ and $perc_{\text{model},i}$ for the M_5seg_TAM and M_5seg models were 0.83 and 56.0% across all conditions respectively. The M_HT model had the smallest $\rho_{\text{model},i}$ (0.70) and $perc_{\text{model},i}$ (32.2%) respectively across all conditions. As shown in 6, there was no significant difference found in $incre_{\text{model},i}$ between the M_7seg_TAM/M_7seg models and the full-body model in all conditions, while all pair-wise comparisons in $incre_{\text{model},i}$ between other simplified models and the full-body model were significantly different.

Pair-wise comparisons of $\rho_{\text{model},i}$, $perc_{\text{model},i}$ and $incre_{\text{model},i}$ between simplified models with and without RAMs of lower body segments indicated no significant difference in most conditions. The M_7seg_TAM model only showed significantly smaller $perc_{\text{model},i}$ in the unperturbed condition than the M_7seg model with a difference of 4.8%, as demonstrated in Fig. 5a. Pair-wise contrasts also detected significant differences between the M_5seg_TAM and M_5seg models in $\rho_{\text{model},i}$, $perc_{\text{model},i}$ in the unperturbed condition (Figs. 4 and 5a). These results provided clear results that the RAMs of the lower limb segments had limited contributions in estimating the sagittal-plane WBAM.

4. Discussion

The aim of this paper is to identify appropriate segments in estimating sagittal-plane WBAM with respect to the whole-body CoM during both unperturbed and perturbed gaits. Those appropriate segments were constructed as a simplified model, and the sagittal-plane WBAM based on a simplified model was calculated by combining the angular momenta of the selected segments. The ideal simplified model should exhibit high $\rho_{\text{model},i}$ (close to 1) and $perc_{\text{model},i}$ (close to 100%) values, and exhibit similar sensitivity ($incre_{\text{model},i}$) to external perturbations as the full-body model. Firstly, to identify the set of segments for the simplified model, we evaluated segmental contributions to the WBAM under the condition of pure sagittal-plane WBAM perturbations. We found that the HT segment and lower limb segments were the major contributors, with the TAMs of lower limb segments being much larger than their RAMs. Based on these major contributing segments, we evaluated several simplified models. Among the models we assessed, the simplified models (the M_7seg_TAM and M_7seg models) with seven segments were proved to be the most effective simplified models for estimating the sagittal-plane WBAM since across all conditions, they provided an average $\rho_{\text{model},i}$ and $perc_{\text{model},i}$ of 0.99 and 96.8% respectively, and their $incre_{\text{model},i}$ both had no significant difference compared to the full-body model.

The separation of RAM and TAM could help us further simplify the models with seven segments, and provide us with an insightful understanding of the importance of different components of segmental angular momenta. Firstly, pair-wise comparisons between the simplified models with and without RAMs of lower body segments indicated no significant difference in most conditions, thus the RAMs of lower limb segments were found to be neglectable, which may simplify the kinematics measurement of lower limbs since we only need to measure the relative positions/velocities between the CoMs of lower limb segments and the whole-body CoM. Therefore, we suggest that the M_7seg_TAM model may be a better choice than the M_7seg model. However, the $perc_{\text{model},i}$ of the M_7seg_TAM model was significantly smaller than the M_7seg model in the unperturbed condition, with a difference of 4.8%. The contributions of RAMs of lower body segments in the unperturbed condition were relatively larger than in perturbed conditions due to the lower contribution of the HT segment in the unperturbed condition (Fig. B3). This may explain the above-mentioned significant difference. Secondly, this separation also helps us to better understand how segmental angular momenta are coordinated (Gaffney et al., 2017).

Table 1
Choice of simplified models, where the set of segments **S** with major contributions was determined based on our segmental contribution analysis results in Appendix B. $a_j \in \{0,1\}, b_j \in \{0,1\}$ with '1' including TAM/RAM of the segment, '0' denoting without including the component. Translational angular momentum (TAM) resulted from the translation of the segment CoM relative to the whole-body CoM, and rotational angular momentum (RAM) resulted from the rotation about its own CoM.

Set of selected segments **S**	HT (head & torso) (including the pelvis)		Thighs		Shanks		Feet	
a_j, b_j	TAM	RAM	TAM	RAM	TAM	RAM	TAM	RAM
M_HT	1	1	0	0	0	0	0	0
M_5seg_TAM	1	1	1	0	1	0	0	0
M_5seg	1	1	1	1	1	1	0	0
M_7seg_TAM	1	1	1	0	1	0	1	0
M_7seg	1	1	1	1	1	1	1	1

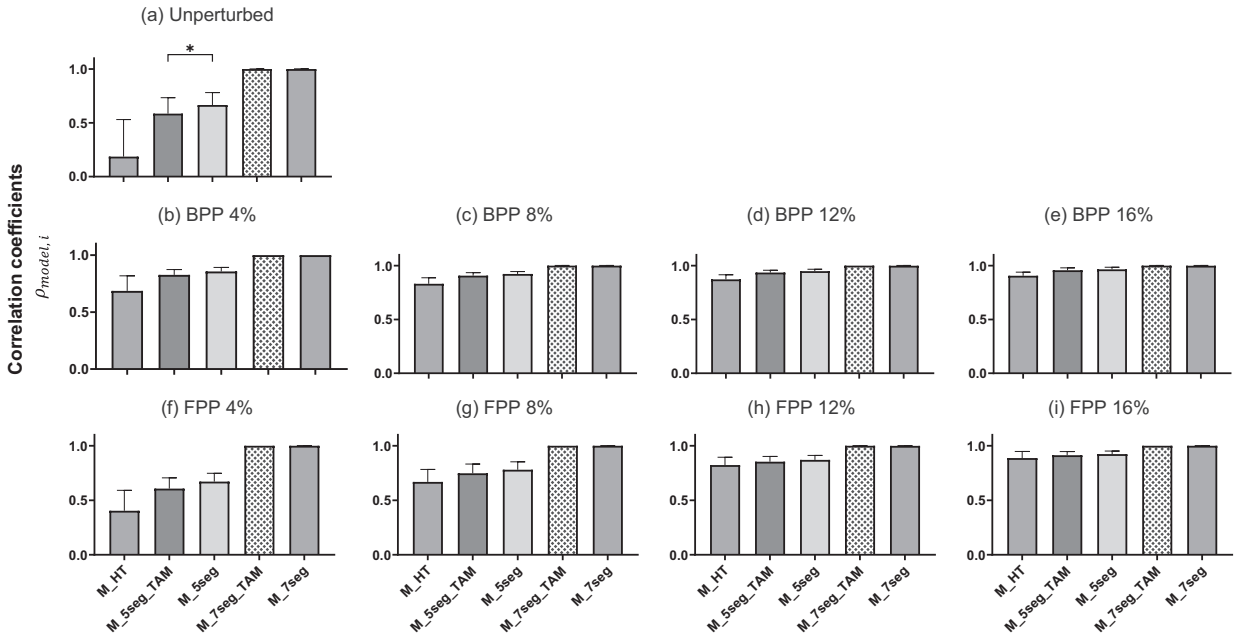

Fig. 4. Mean and SD of the correlation coefficients $\rho_{\text{model},i}$ for simplified models listed in Table 1 that were calculated across all repetitions and subjects during unperturbed and perturbed conditions. Pair-wise comparisons between simplified models with and without RAMs of lower body segments were indicated by '*' representing a significant difference ($p < 0.05$). The forward pitch perturbations (FPP) were defined as backward forces on the pelvis and forward forces on the upper body with equal magnitudes (represented by % of the body weight, % BW), and in the opposite direction for backward pitch perturbations (BPP).

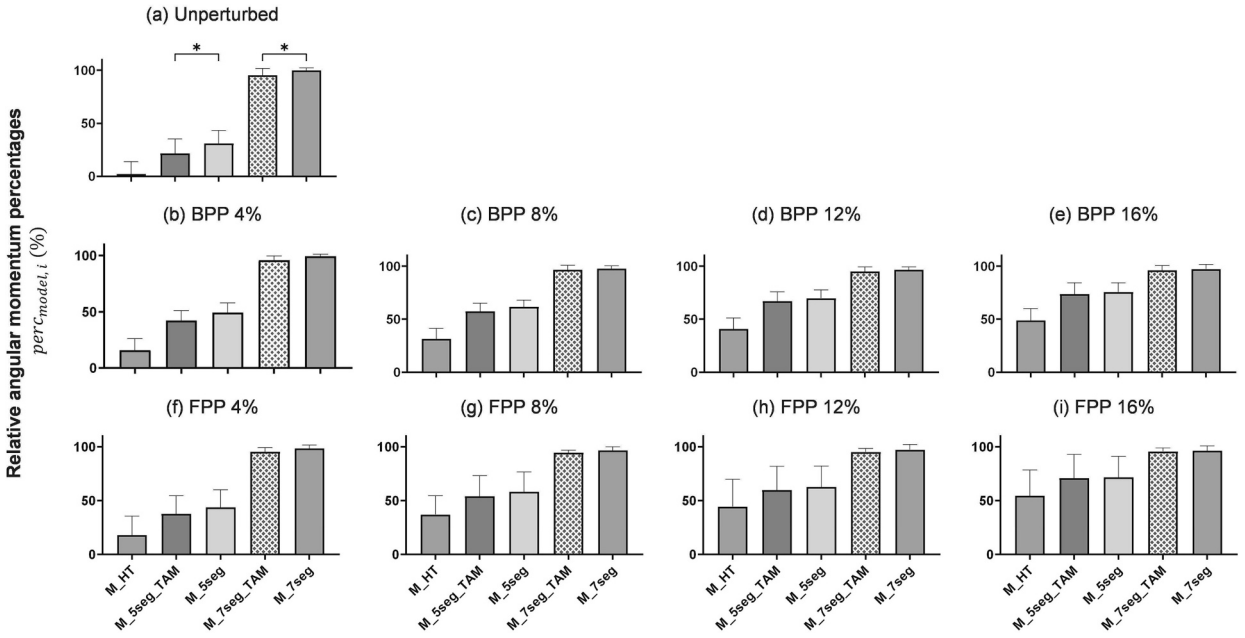

Fig. 5. Mean and SD of the relative angular momentum percentages $perc_{\text{model},i}$ for simplified models listed in Table 1 that were calculated across all repetitions and subjects during unperturbed and perturbed conditions. Pair-wise comparisons between between simplified models with and without RAMs of lower body segments were indicated by '*' representing a significant difference ($p < 0.05$). The forward pitch perturbations (FPP) were defined as backward forces on the pelvis and forward forces on the upper body with equal magnitudes (represented by % of the body weight, % BW), and in the opposite direction for backward pitch perturbations (BPP).

TAMs could help to interpret the segmental dynamics with respect to the whole-body CoM needed to maintain the forward translation

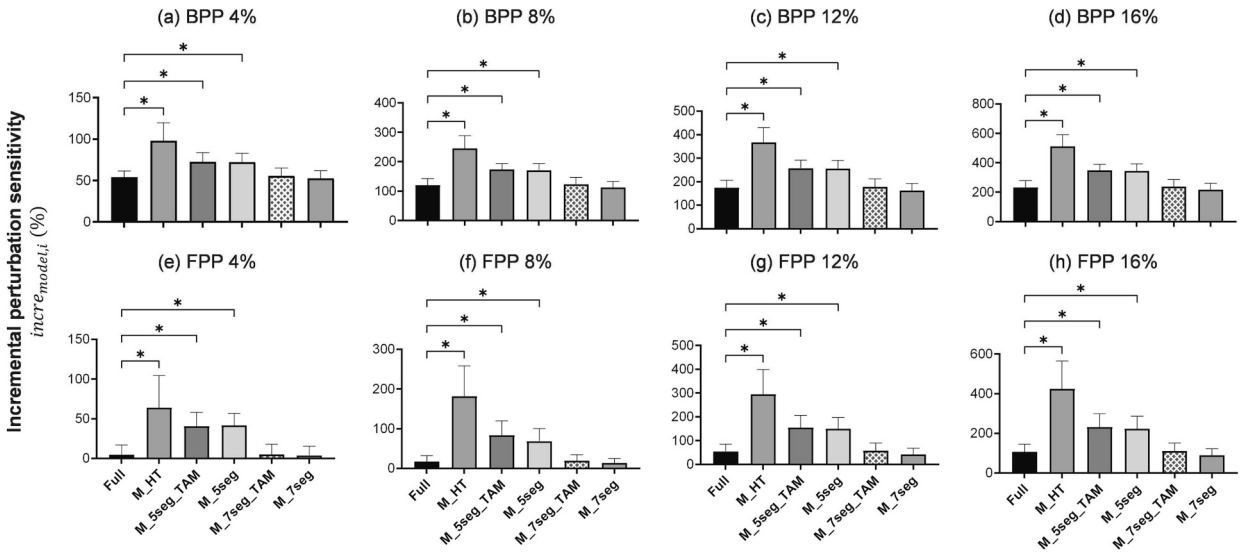

Fig. 6. Mean and SD of the relative angular momentum percentages $incre_{\text{model},i}$ for the full-body model and simplified models listed in Table 1 that were calculated across all repetitions and subjects during unperturbed and perturbed conditions. Pair-wise comparisons between models were indicated by '*' representing a significant difference ($p < 0.05$). The forward pitch perturbations (FPP) were defined as backward forces on the pelvis and forward forces on the upper body with equal magnitudes (represented by % of the body weight, % BW), and in the opposite direction for backward pitch perturbations (BPP).

of the body, while RAMs, generated or arrested by the rotational moments, could be used to provide insight regarding joint kinetics. In sagittal walking, humans move forward primarily through intersegmental coordination among lower limb segments, rather than rotating these segments around their CoMs. This distinction may explain why TAMs from lower limb segments contribute much more to the sagittal-plane WBAM than RAMs.

The potential applicability of the other simplified models in alternative applications is worth considering in future studies. For example, in perturbation or fall detection applications, abrupt deviations in the angular momentum pattern can be used as an indicator of unexpected perturbations (Martelli, Monaco, & Micera, 2011). The key question is to determine a strategy for mapping deviations in angular momentum patterns to perturbations or falls. In such scenarios, a larger incremental perturbation sensitivity ($incre_{\text{model},i}$) could be more beneficial if threshold-based methods were used, for example, using a constant threshold (Martelli et al., 2011) or adaptive thresholds (Bayón et al., 2022; Wang, Raitor, Collins, Liu, & Kennedy, 2023). In the M_HT model, there was no partial cancellation of the angular momentum of the HT segment by other segments that were in the contra phase. Therefore, the M_HT model may prove effective in detecting deviations in the sagittal-plane WBAM caused by perturbations, as evidenced by its larger $incre_{\text{model},i}$ values compared to other simplified models in Fig. 6.

We used Pearson's correlation coefficients and relative angular momentum percentages in our segmental contribution evaluation, which provided clearer insights into the segmental contributions to the WBAM. Previous studies (Herr & Popovic, 2008; Martelli et al., 2013) used the principal component analysis (PCA) to evaluate segmental angular momentum contributions, which is a popular covariance-related method. However, the interpreting of the principal components of PCA is challenging, which made it less straightforward to extract the importance of each segment. Furthermore, PCA only indicates the covariance relationship between the WBAM and segmental angular momenta, potentially resulting in the incorrect identification of major contributing segments. For example, upper limb segments were assigned larger PCA coefficients than the trunk (or chest) (Herr & Popovic, 2008; Martelli et al., 2013), leading to a suggestion that upper limb segments should be included in the simplified body. However, as observed from our results, upper limb segments had much lower contributions to the sagittal-plane WBAM compared to the HT and lower limb segments, thus we could leave the upper limb segments out in the simplified model when we estimated the sagittal-plane WBAM. In other studies, the percentage between the averaged absolute segmental angular momentum and WBAM (Begue et al., 2021), or the percentage between the summed absolute segmental angular momentum and WBAM (Bruijn et al., 2008), was used to determine the relative importance of each segmental angular momentum. However, using absolute values as the evaluation metric could not indicate positive or negative segmental angular momentum contributions, such as the negative contributions of thighs as shown in Figs. B2 and B3. We consider negative contributions to be equally crucial in explaining segment-to-segment cancellation.

Our results were in line with previous findings of the importance of the different segments in regulating the sagittal-plane WBAM (Bennett et al., 2010; Gomez et al., 2022; Herr & Popovic, 2008; Nolasco et al., 2019; Pickle et al., 2014, 2016). The segmental contributions and the potential utility of using the simplified model we proposed for estimating the WBAM in other planes could be explored and speculated through existing literature. Lower limb segments always contributed to the majority of the WBAM, not only in the sagittal plane but also in frontal and transversal planes, during unperturbed walking (Bennett et al., 2010; Herr & Popovic, 2008; Nolasco et al., 2019) and walking with external perturbations (Martelli et al., 2013). As shown previously (Bruijn et al., 2008; Herr & Popovic, 2008), the HT segment showed a less dominant contribution than lower limb segments to the WBAM during unperturbed walking, as humans naturally

maintain an upright head and torso posture in such conditions. However, our experimental results demonstrated a rapid recovery of angular momentum in the HT segment after perturbation, indicating its crucial role in the WBAM recovery and preventing balance loss and fall injuries from unexpected perturbations in the sagittal plane. Given the trunk's large inertia, the HT segment's increasing involvement in the WBAM regulation is not surprising during challenging tasks (Duchene, Mornieux, Petel, Perrin, & Gauchard, 2021) or external perturbations (Sung, Cavataio, & Sauve, 2020), which may also apply for other planes. Upper limb segments, that is, arms, displayed more significant contributions to WBAM in the transverse-plane WBAM than in the sagittal and frontal planes (Bennett et al., 2010; Nolasco et al., 2019). Therefore the seven-seg model without the RAMs of the lower limb segments, which neglects upper limb segments, might be able to also provide accurate WBAM estimations in the frontal plane. However, in the transversal plane, segmental angular momenta of upper limb segments may need to be included and investigated in detail in different daily-life tasks in our future work.

It is also worth exploring how segmental contributions may vary and assessing the feasibility of using a single simplified model to estimate WBAM under different types of perturbations. Unfortunately, only a limited number of studies have delved into similar issues. There were some studies investigating the importance of arms during gait. For example, Pijnappels, Kingma, Wezenberg, Reurink, & Van Dieën, 2010 found that the simplified model ignoring the arms mainly leads to a less adequate body orientation in the transversal plane, Bruijn, Sloot, Kingma, & Pijnappels, 2022 highlighted the positive impact of arm motion on postural stability after tripping, and Collins, Adamczyk, & Kuo, 2009 indicated that the arms contributed to the metabolic cost reduction in walking. Despite the undeniably important role of arms in maintaining human balance, these studies did not specifically investigate the contribution of arms to the recovery of WBAM after perturbations. Arms may still result in limited contributions to the recovery of WBAM due to their relatively small mass and inertia. Based on the fact that the HT segment and lower limb segments have much larger mass and inertia than arms, we anticipate that the HT segment and lower limb segments will continue to be primary contributors to WBAM in other perturbation scenarios.

5. Limitations and future work

Our work is the first to examine the performance of simplified models for WBAM estimation based on segmental contributions, both in unperturbed and perturbed conditions. In our experiments, participants walked on a treadmill in the sagittal plane, with only the WBAM being perturbed. As previously mentioned, in order to comprehensively assess the feasibility of utilizing a single simplified model, it is necessary in our future work to evaluate its performance in estimating the WBAM in other planes and under various types of perturbations like stumbling or slipping, or other daily-life conditions (Geerse, Roerdink, Marinus, & van Hilten, 2019). Furthermore, we only evaluated the impact of WBAM perturbations in the sagittal plane, we do not know its impact on the balance control in the frontal plane. Previous papers (Bauby & Kuo, 2000; Kuo & Donelan, 2010; Rosenblatt & Grabiner, 2010) discussed the importance of balance control in the frontal plane while the direction of walking was only directed in the sagittal plane. A disruption of the sagittal-plane WBAM during sagittal-plane activities may still influence the WBAM in the frontal plane. This will also be evaluated in our future work including 3-D data in other planes and during other daily-life conditions.

In our simplified model, we dropped out the segmental angular momenta of upper limb segments. It is also interesting to investigate whether it will be possible to enhance the performance of the simplified model in estimating the WBAM, if the angular momenta of upper limb segments are transferred to the body by adding their mass and inertia to the HT segment. Additionally, as mentioned in (3) in **Section 2.4 Evaluation method**, the position and velocity of the whole-body CoM used in computing the WBAM based on the simplified models were the same as the values computed from the full-body model. In future work, we should also consider the impact of the exclusion of upper limb segments on the whole-body CoM position and velocity calculation (Schinkel-Ivy, Komisar, & Duncan, 2020) when we used the simplified model with seven segments.

6. Conclusion

In summary, our study indicates that we were able to estimate the sagittal-plane WBAM with respect to the whole-body CoM from a reduced set of segments. The reduced set of segments was constructed as a simplified model, and the sagittal-plane WBAM based on a simplified model was calculated by combining the angular momenta of the selected segments. Among the simplified models we evaluated, seven-seg models including the HT and lower limb segments provided the best performance (with an average correlation coefficient of 0.99 and relative angular momentum percentage of 96.8%) and exhibited the most similar sensitivity to external perturbations as the full-body model. The selection of segments for the simplified models was motivated by detailed segmental angular momentum contribution analysis, which revealed that the HT and lower limb segments were the major contributors to the sagittal-plane WBAM. Additionally, we found that ignoring the RAMs of lower limb segments had a negligible effect on the performance of the simplified models. These findings are expected to have practical implications for the development of IMU-based solutions for estimating WBAM, as they may help reduce the number of required sensors and simplify kinematics measurement.

CRediT authorship contribution statement

J. Zhang: Writing – review & editing, Writing – original draft, Visualization, Validation, Software, Methodology, Investigation, Formal analysis, Data curation, Conceptualization. **M. van Mierlo:** Writing – review & editing, Validation, Software, Resources, Methodology, Data curation. **P.H. Veltink:** Writing – review & editing, Validation, Supervision, Resources, Methodology, Conceptualization. **E.H.F. van Asseldonk:** Writing – review & editing, Validation, Supervision, Resources, Project administration, Methodology, Funding acquisition, Conceptualization.

Declaration of competing interest

The authors declare that they have no competing or financial interests.

Data availability

The data will be published in 4TU.Research Data with a DOI attached in the final paper.

Acknowledgements

This paper has been supported in part by the research program Wearable Robotics with project number P16-05 funded by the Dutch Research Council (NWO) and the scholarship that Junhao Zhang received from China Scholarship Council (CSC No. 202008330287), whose assistance is gratefully acknowledged.

Appendix A. Evaluation method on segmental angular momentum contributions

The angular momenta of the left and right limbs were added together to evaluate the segmental angular momentum contributions. This leads to a set of 8 segmental angular momenta, $H_{seg,k}, k = 1,\ldots,8$. They are the angular momenta of the pelvis, HT, and the sum of the angular momenta of left and right thighs, shanks, feet, upper arms, forearms, and hands. Within one stride cycle, the segmental angular momentum contributions were evaluated in comparison to the estimated WBAM both in terms of pattern similarity (using Pearson's correlation coefficients) and magnitude. The Pearson's correlation coefficient of each segmental angular momentum was defined as $\rho_{seg,k}^{\text{overall}}$. To determine the segmental angular momentum contribution in magnitude, we took the median of the relative angular momentum percentages between segmental angular momentum and the WBAM within one stride cycle,

$$perc_{seg,k}^{\text{overall}} = \underset{t=1,2,\ldots,100}{\text{Median}}\left[\frac{H_{seg,k}(t)}{H_{\text{full}}(t)}\right] \times 100\% \tag{A1}$$

As shown in (A1), we conducted a segmental angular momentum contribution analysis for the overall segmental angular momentum, as well as separately for TAM and RAM, by comparing them with the WBAM. The notations of Pearson's correlation coefficients and relative angular momentum percentages for TAM and RAM were $\rho_{seg,k}^{\text{RAM}}$, $\rho_{seg,k}^{\text{TAM}}$, $perc_{seg,k}^{\text{RAM}}$, and $perc_{seg,k}^{\text{TAM}}$.

Appendix B. Segmental angular momentum contribution results

Fig. B1 shows the WBAM and segmental angular momenta under the unperturbed, BPP 12% and FPP 12% conditions, including the overall angular momenta, RAMs and TAMs. Meanwhile, Fig. B2 and Fig. B3 display the mean and SD of $\rho_{seg,k}^{\text{overall}}$, $\rho_{seg,k}^{\text{RAM}}$, $\rho_{seg,k}^{\text{TAM}}$, and $perc_{seg,k}^{\text{overall}}$, $perc_{seg,k}^{\text{RAM}}$, $perc_{seg,k}^{\text{TAM}}$ for each segment.

The HT segment and lower limb segments were major contributing segments. Shanks and feet both had large $\rho_{seg,k}^{\text{overall}}$ and $perc_{seg,k}^{\text{overall}}$ across all conditions, which definitely made them major contributing segments. Although thighs and the HT segment did not always have large$\rho_{seg,k}^{\text{overall}}$ and $perc_{seg,k}^{\text{overall}}$, they were still selected as major contributing segments. In the unperturbed or perturbed conditions with small magnitudes (such as FPP8% and BPP4% conditions), $\rho_{seg,k}^{\text{overall}}$ and $perc_{seg,k}^{\text{overall}}$ of the thighs were negative. These large negative $\rho_{seg,k}^{\text{overall}}$ or $perc_{seg,k}^{\text{overall}}$ indicated that the thighs induced large segmental cancellation under these conditions, which cannot be ignored. Under the unperturbed condition, the HT segment had a low $\rho_{seg,k}^{\text{overall}}$ of 0.19 (Fig. B2a-2) and $perc_{seg,k}^{\text{overall}}$ of 2.5% (Fig. B3a-2). However, as perturbation magnitudes increased from 4% BW to 16% BW, its contribution increased from 0.45 to 0.90 for $\rho_{seg,k}^{\text{overall}}$, and from 16.9% to 51.6% for $perc_{seg,k}^{\text{overall}}$, averaging across BPP and FPP. Furthermore, as shown in Fig. B1, after the perturbation finished, the segmental angular momentum of the HT segment recovered to normal values very soon. These results indicated that the HT segment played an important role in the regulation of the WBAM under WBAM perturbations. On the contrary, although the pelvis and upper limb segments provided large $\rho_{seg,k}^{\text{overall}}$ in many conditions, their $perc_{seg,k}^{\text{overall}}$ were small under all conditions (Fig. B3a-1), ranging from only −3.3% to 1.7% for pelvis and being <2% for upper limb segments, thus they were ignored in simplified models.

Furthermore, the TAMs of lower limb segments comprised the most to segmental angular momenta, regardless of whether the conditions were perturbed or not (Fig. B1g i, Fig. B3c-1 c-8). Therefore, in the following analysis, we compared the simplified models with and without the RAMs of lower limb segments to test whether the RAMs of lower limb segments could be ignored. This was not the case for the HT segment. When there was no perturbation, the RAM of the HT segment showed negative $\rho_{seg,k}^{\text{overall}}$ and $perc_{seg,k}^{\text{overall}}$, while those of the TAM were positive. Under perturbed conditions, the TAM and RAM of the HT segment were almost equal.

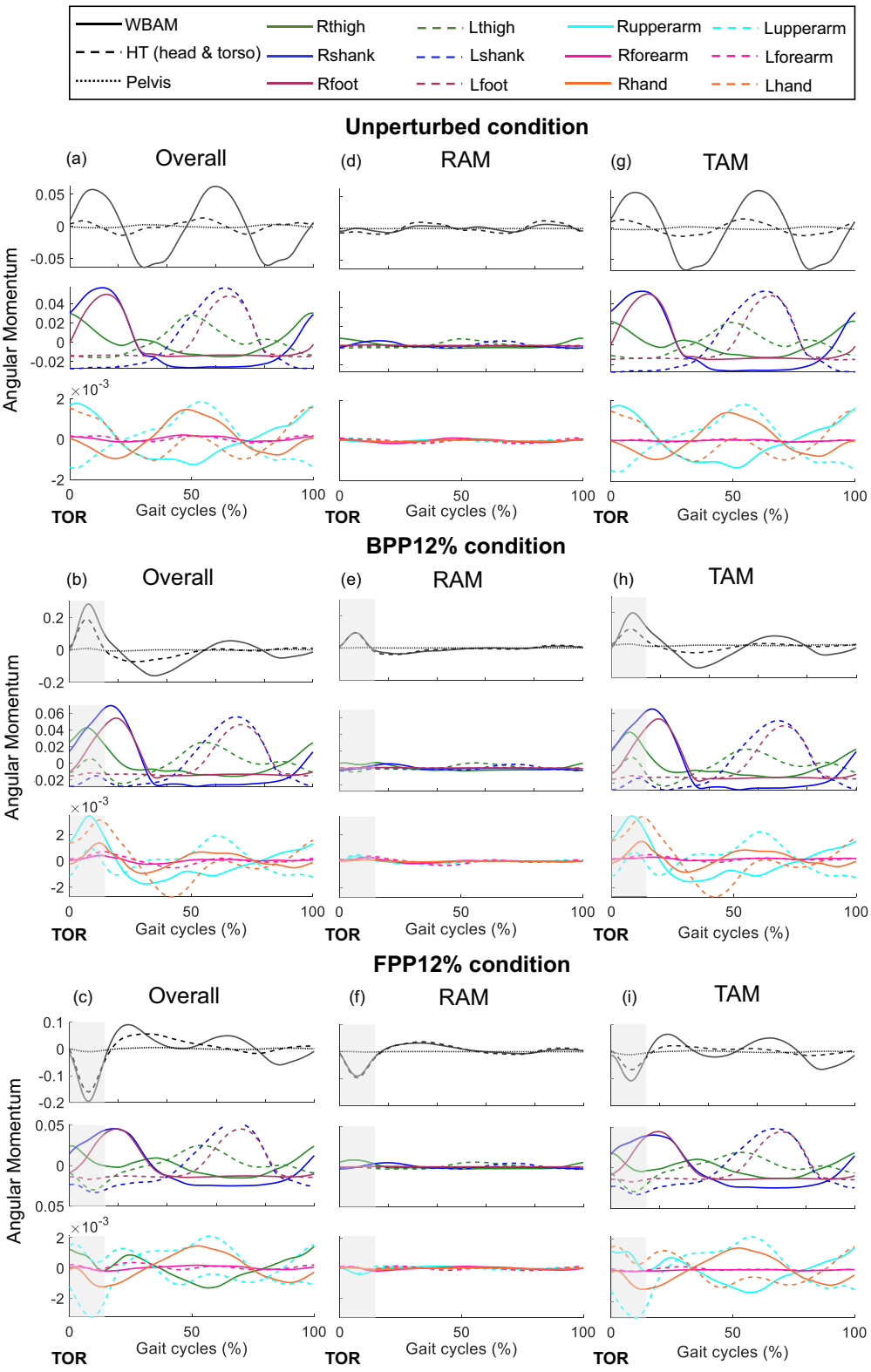

Fig. B1. Averaged normalized sagittal-plane whole-body angular momentum (WBAM) H_{full} and segmental angular momenta H_j across all repetitions and subjects under the unperturbed, BPP12% and FPP12% conditions. The overall angular momenta (a-c), RAM (d-f), and TAM (g-i) of the full-body model and each segment are shown. Translational angular momentum (TAM) and rotational angular momentum (RAM) are the two components of the overall angular momentum. TAM results from the translation of the segment CoM relative to the whole-body CoM, and RAM results

from the rotation about its own CoM. The forward pitch perturbations (FPP) were defined as backward forces on the pelvis and forward forces on the upper body with equal magnitudes (represented by % of the body weight, % BW), and in the opposite direction for backward pitch perturbations (BPP). Perturbations were given at the moment of toe-off right (TOR) and lasted for 150 ms with the gray shaded area representing the perturbation period.

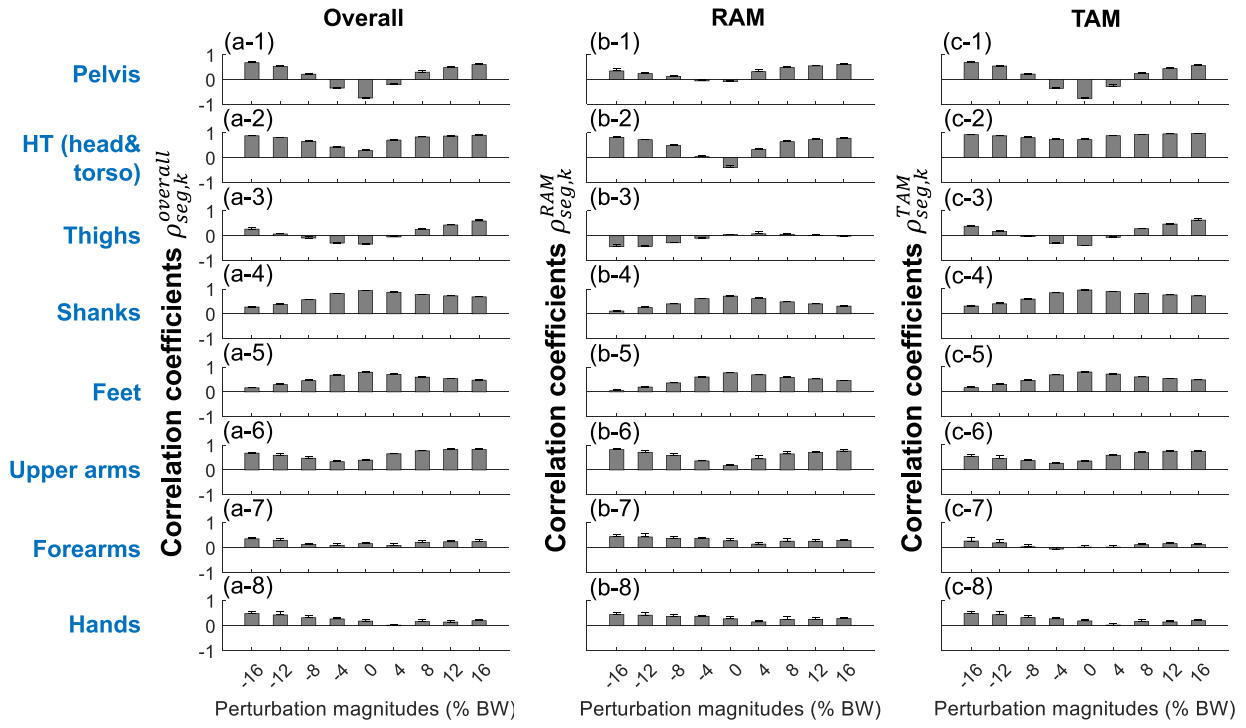

Fig. B2. Mean and SD of the correlation coefficients $\rho_{seg.k}^{\text{overall}}$ (a-1∼a-8), $\rho_{seg.k}^{\text{RAM}}$ (b-1∼b-8), and $\rho_{seg.k}^{\text{TAM}}$ (c-1∼c-8) of segments that were calculated across all repetitions and subjects, under all the unperturbed and perturbed conditions. Translational angular momentum (TAM) and rotational angular momentum (RAM) are the two components of the overall angular momentum. TAM results from the translation of the segment CoM relative to the whole-body CoM, and RAM results from the rotation about its own CoM. Perturbations were represented by % body weight (% BW) with positive values as the backward pitch perturbations (FPP) and negative values as forward pitch perturbations (FPP).

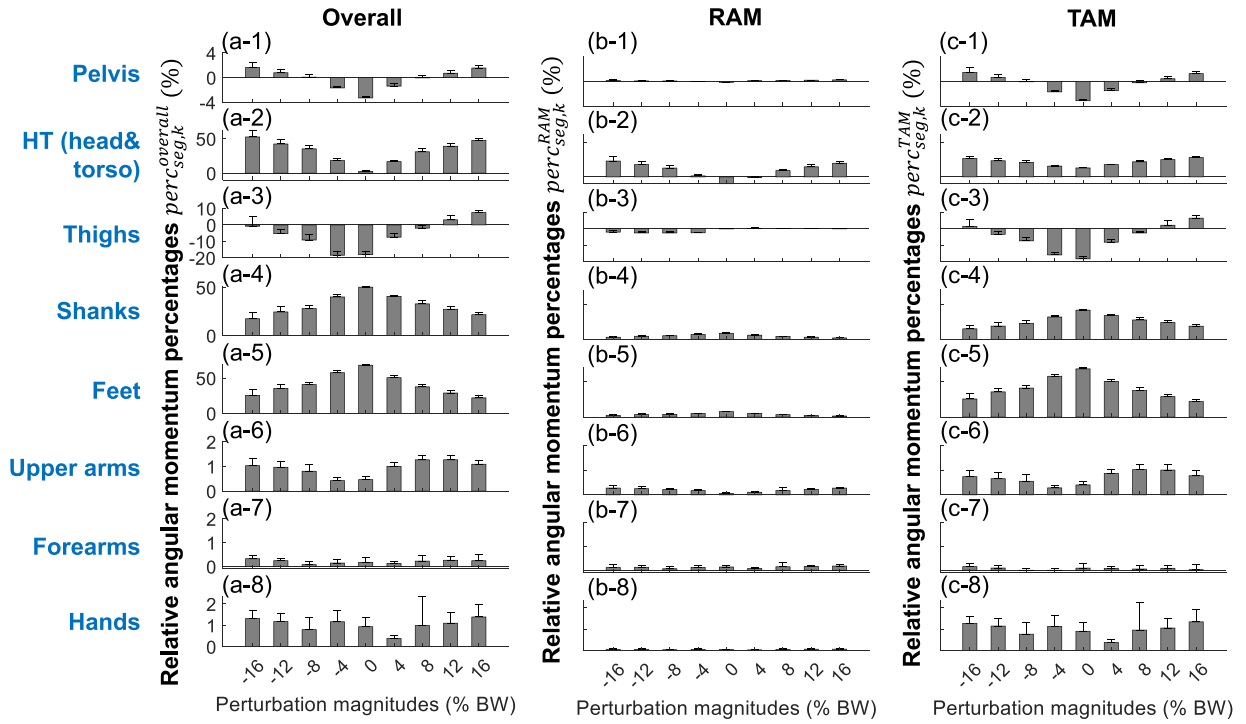

Fig. B3. Mean and SD of the relative angular momentum percentages $perc_{seg.k}^{\text{overall}}$ (a-1∼a-8), $perc_{seg.k}^{\text{RAM}}$ (b-1∼b-8), and $perc_{seg.k}^{\text{TAM}}$ (c-1∼c-8) of segments that were calculated across all repetitions and subjects, under all the unperturbed and perturbed conditions. Translational angular momentum (TAM) and rotational angular momentum (RAM) are the two components of the overall angular momentum. TAM results from the translation of the segment CoM relative to the whole-body CoM, and RAM results from the rotation about its own CoM. Perturbations were represented by % body weight (% BW) with positive values as the backward pitch perturbations (FPP) and negative values as forward pitch perturbations (FPP).

References

Bauby, C. E., & Kuo, A. D. (2000). Active control of lateral balance in human walking. *Journal of Biomechanics, 33*(11), 1433–1440. https://doi.org/10.1016/s0021-9290(00)00101-9

Bayón, C., Keemink, A. Q. L., van Mierlo, M., Rampeltshammer, W., van der Kooij, H., & van Asseldonk, E. H. F. (2022). Cooperative ankle-exoskeleton control can reduce effort to recover balance after unexpected disturbances during walking. *Journal of Neuroengineering and Rehabilitation, 19*(1), 21. https://doi.org/10.1186/s12984-022-01000-y

Begue, J., Peyrot, N., Lesport, A., Turpin, N. A., Watier, B., Dalleau, G., & Caderby, T. (2021). Segmental contribution to whole-body angular momentum during stepping in healthy young and old adults. *Scientific Reports, 11*(1), 19969. https://doi.org/10.1038/s41598-021-99519-y

Bennett, B. C., Russell, S. D., Sheth, P., & Abel, M. F. (2010). Angular momentum of walking at different speeds. *Human Movement Science, 29*(1), 114–124. https://doi.org/10.1016/j.humov.2009.07.011

Brough, L. G., Klute, G. K., & Neptune, R. R. (2021). Biomechanical response to mediolateral foot-placement perturbations during walking. *Journal pf Biomechanics, 116*, Article 110213. https://doi.org/10.1016/j.jbiomech.2020.110213

Bruijn, S. M., Meijer, O. G., van Dieën, J. H., Kingma, I., & Lamoth, C. J. (2008). Coordination of leg swing, thorax rotations, and pelvis rotations during gait: The organisation of total body angular momentum. *Gait & Posture, 27*(3), 455–462. https://doi.org/10.1016/j.gaitpost.2007.05.017

Bruijn, S. M., Meyns, P., Jonkers, I., Kaat, D., & Duysens, J. (2011). Control of angular momentum during walking in children with cerebral palsy. *Research in Developmental Disabilities, 32*(6), 2860–2866. https://doi.org/10.1016/j.ridd.2011.05.019

Bruijn, S. M., Sloot, L. H., Kingma, I., & Pijnappels, M. (2022). Contribution of arm movements to balance recovery after tripping in older adults. *Journal of Biomechanics, 133*, Article 110981. https://doi.org/10.1016/j.jbiomech.2022.110981

Collins, S. H., Adamczyk, P. G., & Kuo, A. D. (2009). Dynamic arm swinging in human walking. *Proceedings. Biological sciences, 276*(1673), 3679–3688. https://doi.org/10.1098/rspb.2009.0664

Duchene, Y., Mornieux, G., Petel, A., Perrin, P. P., & Gauchard, G. C. (2021). The trunk's contribution to postural control under challenging balance conditions. *Gait & Posture, 84*, 102–107. https://doi.org/10.1016/j.gaitpost.2020.11.020

Dunn, O. J. (1964). Multiple comparisons using rank sums. *Technometrics, 6*(3), 241–252. https://doi.org/10.1080/00401706.1964.10490181

Friedman, M. (1940). A comparison of alternative tests of significance for the problem of *m* rankings. *The Annals of Mathematical Statistics, 11*(1), 86–92. https://doi.org/10.1214/aoms/1177731944

Gaffney, B. M., Christiansen, C. L., Murray, A. M., Silverman, A. K., & Davidson, B. S. (2017). Separation of rotational and translational segmental momentum to assess movement coordination during walking. *Human Movement Science, 51*, 99–111. https://doi.org/10.1016/j.humov.2016.12.001

Gaffney, B. M. M., Christiansen, C. L., Murray, A. M., & Davidson, B. S. (2017). Trunk kinetic effort during step ascent and descent in patients with transtibial amputation using angular momentum separation. *Clinical Biomechanics (Bristol, Avon), 48*, 88–96. https://doi.org/10.1016/j.clinbiomech.2017.07.014

Geerse, D. J., Roerdink, M., Marinus, J., & van Hilten, J. J. (2019). Walking adaptability for targeted fall-risk assessments. *Gait & Posture, 70*, 203–210. https://doi.org/10.1016/j.gaitpost.2019.02.013

Gomez, N. G., Foreman, K. B., Hunt, M., & Merryweather, A. S. (2022). Regulation of whole-body and segmental angular momentum in persons with parkinson's disease on an irregular surface. *Clinical Biomechanics (Bristol, Avon), 99*, Article 105766. https://doi.org/10.1016/j.clinbiomech.2022.105766

Herr, H., & Popovic, M. (2008). Angular momentum in human walking. *Journal of Experimental Biology, 211*(Pt 4), 467–481. https://doi.org/10.1242/jeb.008573

Honda, K., Sekiguchi, Y., Muraki, T., & Izumi, S. I. (2019). The differences in sagittal plane whole-body angular momentum during gait between patients with hemiparesis and healthy people. *Journal of Biomechanics, 86*, 204–209. https://doi.org/10.1016/j.jbiomech.2019.02.012

van der Kooij, H., Fricke, S. S., Veld, R. C. V., Prieto, A. V., Keemink, A. Q. L., Schouten, A. C., & van Asseldonk, E. H. F. (2022). Identification of hip and knee joint impedance during the swing phase of walking. *IEEE Transactions on Neural Systems and Rehabilitation Engineering, 30*, 1203–1212. https://doi.org/10.1109/TNSRE.2022.3172497

Kuo, A. D., & Donelan, J. M. (2010). Dynamic principles of gait and their clinical implications. *Physical Therapy, 90*(2), 157–174. https://doi.org/10.2522/ptj.20090125

de Leva, P. (1996). Adjustments to zatsiorsky-seluyanov's segment inertia parameters. *Journal of Biomechanics, 29*(9), 1223–1230. https://doi.org/10.1016/0021-9290(95)00178-6

Liu, M., Naseri, A., Lee, I.-C., Hu, X., Lewek, M. D., & Huang, H. (2023). A simplified model for whole-body angular momentum calculation. *Medical Engineering and Physics, 111*, Article 103944. https://doi.org/10.1016/j.medengphy.2022.103944

Martelli, D., Monaco, V., Bassi Luciani, L., & Micera, S. (2013). Angular momentum during unexpected multidirectional perturbations delivered while walking. *IEEE Transactions on Biomedical Engineering, 60*(7), 1785–1795. https://doi.org/10.1109/tbme.2013.2241434

Martelli, D., Monaco, V., & Micera, S. (2011). Detecting falls by analyzing angular momentum. *IEEE International Conference on Rehabilitation Robotics, 2011*, 5975404. https://doi.org/10.1109/icorr.2011.5975404

van Mierlo, M., Ambrosius, J. I., Vlutters, M., van Asseldonk, E. H. F., & van der Kooij, H. (2022). Recovery from sagittal-plane whole body angular momentum perturbations during walking. *Journal of Biomechanics, 141*, Article 111169. https://doi.org/10.1016/j.jbiomech.2022.111169

Millard, M., Wight, D., McPhee, J., Kubica, E., & Wang, D. (2009). Human foot placement and balance in the sagittal plane. *Journal of Biomechanical Engineering, 131*(12), Article 121001. https://doi.org/10.1115/1.4000193

Miller, S. E., Segal, A. D., Klute, G. K., & Neptune, R. R. (2018). Hip recovery strategy used by below-knee amputees following mediolateral foot perturbations. *Journal of Biomechanics, 76*, 61–67. https://doi.org/10.1016/j.jbiomech.2018.05.023

Nolasco, L. A., Silverman, A. K., & Gates, D. H. (2019). Whole-body and segment angular momentum during 90-degree turns. *Gait & Posture, 70*, 12–19. https://doi.org/10.1016/j.gaitpost.2019.02.003

Nott, C. R., Neptune, R. R., & Kautz, S. A. (2014). Relationships between frontal-plane angular momentum and clinical balance measures during post-stroke hemiparetic walking. *Gait & Posture, 39*(1), 129–134. https://doi.org/10.1016/j.gaitpost.2013.06.008

Pickle, N. T., Wilken, J. M., Aldridge, J. M., Neptune, R. R., & Silverman, A. K. (2014). Whole-body angular momentum during stair walking using passive and powered lower-limb prostheses. *Journal of Biomechanics, 47*(13), 3380–3389. https://doi.org/10.1016/j.jbiomech.2014.08.001

Pickle, N. T., Wilken, J. M., Aldridge Whitehead, J. M., & Silverman, A. K. (2016). Whole-body angular momentum during sloped walking using passive and powered lower-limb prostheses. *Journal of Biomechanics, 49*(14), 3397–3406. https://doi.org/10.1016/j.jbiomech.2016.09.010

Pijnappels, M., Kingma, I., Wezenberg, D., Reurink, G., & Van Dieën, J. H. (2010). Armed against falls: The contribution of arm movements to balance recovery after tripping. *Experimental Brain Research, 201*, 689–699. https://doi.org/10.1007/s00221-009-2088-7

Rajagopal, A., Dembia, C. L., DeMers, M. S., Delp, D. D., Hicks, J. L., & Delp, S. L. (2016). Full-body musculoskeletal model for muscle-driven simulation of human gait. *IEEE Transactions on Biomedical Engineering, 63*(10), 2068–2079. https://doi.org/10.1109/TBME.2016.2586891

Roetenberg, D., Luinge, H., Slycke, P., et al. (2009). Xsens mvn: Full 6dof human motion tracking using miniature inertial sensors. *Xsens motion technologies BV. Technical Report, 1*, 1–7.

Rosenblatt, N. J., & Grabiner, M. D. (2010). Measures of frontal plane stability during treadmill and overground walking. *Gait & Posture, 31*(3), 380–384. https://doi.org/10.1016/j.gaitpost.2010.01.002

Schinkel-Ivy, A., Komisar, V., & Duncan, C. A. (2020). Quantifying segmental contributions to center-of-mass motion during dynamic continuous support surface perturbations using simplified estimation models. *Journal of Applied Biomechanics, 36*(4), 198–208. https://doi.org/10.1123/jab.2019-0239

Sheehan, R. C., Beltran, E. J., Dingwell, J. B., & Wilken, J. M. (2015). Mediolateral angular momentum changes in persons with amputation during perturbed walking. *Gait & Posture, 41*(3), 795–800. https://doi.org/10.1016/j.gaitpost.2015.02.008

Silverman, A. K., Neptune, R. R., Sinitski, E. H., & Wilken, J. M. (2014). Whole-body angular momentum during stair ascent and descent. *Gait & Posture, 39*(4), 1109–1114. https://doi.org/10.1016/j.gaitpost.2014.01.025

Silverman, A. K., Wilken, J. M., Sinitski, E. H., & Neptune, R. R. (2012). Whole-body angular momentum in incline and decline walking. *Journal of Biomechanics, 45*(6), 965–971. https://doi.org/10.1016/j.jbiomech.2012.01.012

Sung, P. S., Cavataio, M., & Sauve, J. (2020). Adaptive trunk sway velocities following repeated perturbations in subjects with and without low back pain. *Journal of Electromyography and Kinesiology, 52*, Article 102423. https://doi.org/10.1016/j.jelekin.2020.102423

Wang, W., Raitor, M., Collins, S., Liu, C. K., & Kennedy, M. (2023). Trajectory and sway prediction towards fall prevention. *IEEE International Conference on Robotics and Automation (ICRA), 2023*, 10483–10489. https://doi.org/10.1109/ICRA48891.2023.10161361

Zatsiorsky, V., & Seluyanov, V. N. (1979). Mass-inertial characteristics of the segments of the human body and their relationship with anthropometric landmarks. *Voprosy Antropologii, 62*, 91–103.